Stereoselective synthesis and structural analysis of polycyclic lactams derived from tetrahydroisoquinoline 1,2- and 1,3-diamines

Henri Kivelä,[a,]* Olli Martiskainen,[a] Kalevi Pihlaja,[a] Zita Zalán,[b] and László Lázár [b,]*

[a] *Department of Chemistry, Structural Chemistry Group, University of Turku, FI-20014, Finland*
[b] *Institute of Pharmaceutical Chemistry, University of Szeged, Eötvös u. 6., H-6720 Szeged, Hungary*
E-mail: hemiki@utu.fi, lazar@pharm.u-szeged.hu

Dedicated to Professor Ferenc Fülöp on the occasion of his 60th birthday

Abstract

By means of the domino ring-closure reactions of (1*S**,1′*S**)-1-(1′-aminoethyl)-, (1*R**,1′*R**)-1-(2′-amino-1′-methylethyl)- and 1-(2-aminophenyl)-6,7-dimethoxy-1,2,3,4-tetrahydroisoquinoline with acyclic and aromatic γ- or δ-oxo acids, angularly-condensed tetra-, penta- and hexacyclic lactam derivatives were formed with practically full diastereoselectivities (*de* ~100%), containing the substituents at the annelations of the saturated heterocyclic rings in *cis* position. The structure and relative stereochemistry of the products were determined with ^{1}H and ^{13}C NMR spectroscopy. Further, the tetrahydropyridine ring (ring B) was observed to prefer *cis* fusion with the condensed imidazolidine or hexahydropyrimidine ring (ring C), with one exception preferring *trans* fusion (namely, the tetracyclic imidazolidine derivative bearing a methyl substituent at the C/D ring annelation, cmpd. **11**). These two conformations can interconvert *via* simultaneous nitrogen inversion at the B/C annelation and ring inversion of the ring B, and their populations could be roughly estimated from the *J*-coupling constant data for each lactam derivative. The compounds gave fragment ions that were typical for the structures of the compounds.

Keywords: Diamine, isoquinoline, lactam, domino reaction, ^{1}H and ^{13}C NMR, electron impact mass spectrometry

Introduction

The cyclocondensation of various 1,2-difunctional compounds (**1**, amino alcohols, amino thiols or diamines, containing a primary amino group) comprise a well-established method for the preparation of 1,3-heterocycle-fused γ- or δ-lactams with a nitrogen at the annelation (**4**).[1] The reaction is classified as a domino process,[2] since it presumably occurs in two steps: first a ring-chain tautomeric intermediate (**3A**-**3B**) is formed, the equilibrium of which gradually shifts towards the cyclic form **4** in consequence of the practically irreversible intramolecular *N*-acylation.[3] The nitrogen-bridged γ- or δ-lactams **4**, both in racemic and in enantiomerically pure form, are often applied as intermediates in numerous synthetic processes involving various regio- and stereocontrolled transformations.[4]

We recently described the domino ring-closures of 1-(aminomethyl)- and 1-(2-aminoethyl)-6,7-dimethoxy-1,2,3,4-tetrahydroisoquinoline with γ- and δ-oxo acids, whereby tetra- and pentacyclic either angularly or linearly tetrahydroisoquinoline-condensed lactam derivatives were formed with excellent diastereoselectivities.[5] As a continuation of this work and in connection with our previous studies on the synthesis and structural analysis of tetrahydroisoquinoline-condensed saturated heterocycles,[6] we now report on the reactions of 1-substituted 1,2,3,4-tetrahydroisoquinoline 1,2- and 1,3-diamines, bearing a methyl substituent or an aromatic ring in the side chain, with γ- and δ-oxo acids. Our aim was to investigate the effects of the side chain substituents and the size of the lactam rings formed on the stereochemical outcome of the reactions, and the conformational and mass spectral behaviour of the tetra- and pentacyclic products.

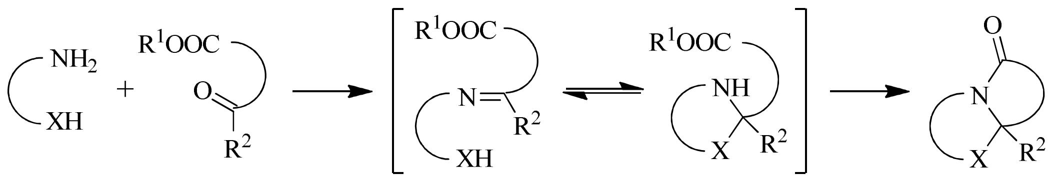

1 **2** **3A** **3B** **4**

X = O, S, NR; R^1 = H, alkyl; R^2 = H, alkyl, aryl

Scheme 1

Results and Discussion

Synthesis

From the starting diamines for the preparation of the target polycyclic lactams, (1*R**,1′*R**)-1-(2′-amino-1′-methylethyl)-6,7-dimethoxy-1,2,3,4-tetrahydroisoquinoline[7] (**10**) and 1-(2-amino-phenyl)-6,7-dimethoxy-1,2,3,4-tetrahydroisoquinoline[8] (**21**) were synthesized according to known procedures. (1*S**,1′*S**)-1-(1′-Aminoethyl)-6,7-dimethoxy-1,2,3,4-tetrahydroisoquinoline (**9**) was prepared in five steps, similarly to its homologue **10**, starting from *N*-Cbz-DL-alanine (**5**) and homoveratrylamine (Scheme 2). Reduction of **7** with $NaBH_4$ gave a *ca*. 8:1 mixture of tetrahydroisoquinoline diastereomers **8a** and **8b**, from which **8a** could be obtained by crystallization and was converted to the 1*S**,1′*S** diamine diastereomer **9**. Diastereomeric ratios

8a:8b were determined from the [1]H NMR spectra by integration of the well separated 1′-Me doublets. The relative configuration of **9** was deduced based on its ring-closed lactam derivatives (see below).[9]

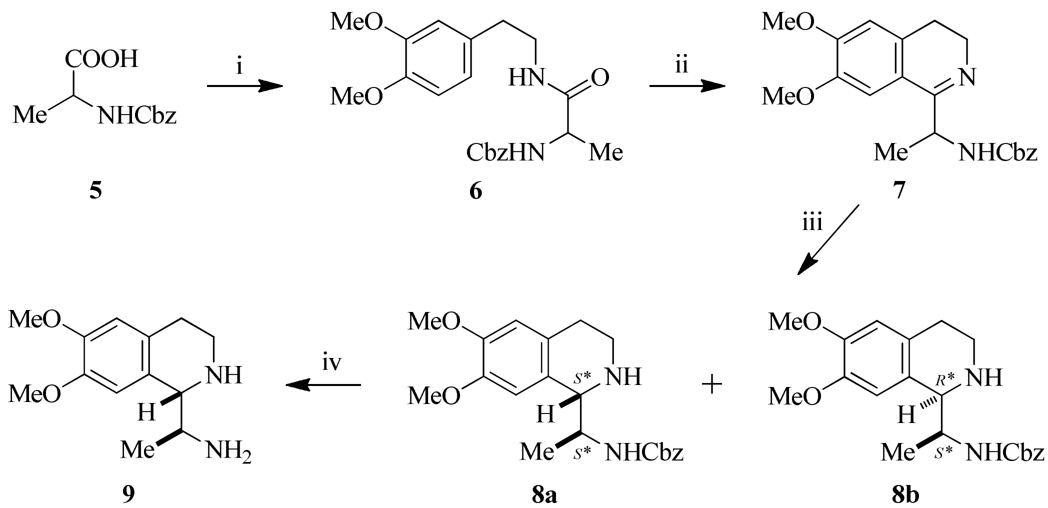

Scheme 2. *Reagents and conditions:* (i) 1: Et_3N, ClCOOEt, toluene, -10 ºC, 5 min, 2. homoveratrylamine, CH_2Cl_2, 0 ºC then reflux, 5 min, 79%; (ii): $POCl_3$, $CHCl_3$, reflux, 3 h, 75%; (iii): $NaBH_4$, MeOH, 0 ºC, 3 h, then r.t., 3 h, **8a**:**8b** = 8:1, **8a**: 74%; (iv): 33% HBr in AcOH, r.t., 30 min, then NaOH, 83%.

When tetrahydroisoquinoline diamines **9** and **10** were boiled in toluene with 4-oxopentanoic acid, 3-benzoylpropanoic acid, 4-benzoylbutanoic acid, 2-formylbenzoic acid or 2-benzoyl-benzoic acid, cyclocondensations generally took place within 2-12 h to furnish the corresponding angularly-condensed tetra- and pentacyclic lactams **11-20** (Scheme 3) in good yields. By a similar reaction of diamine **21** and 2-formylbenzoic acid, the angularly-condensed hexacyclic lactam **22** was obtained (Scheme 4). NMR spectra of the crude products **11-20** and **22** indicated that neither the methyl substituent nor the aromatic ring at the side chain influenced significantly the stereochemical outcome of the lactam formation, since the polycycles **11-20** and **22** were formed with practically full diastereoselectivity (*de* ~100%), affording only the isomers having the hydrogen at the annelation of the tetrahydroisoquinoline and imidazolidine/hexahydro-pyrimidine rings (H-10b for **11-14**, H-11b for **15** and **16**, H-4b for **17-20** and **22**) and substituent R (H at 14b in **22**) in the *cis* position. The observed high *de* values in favour of the formation of the *cis* lactams can be explained as a result of the kinetic control governing the second cyclization steps of the domino cyclocondensations.[3,5]

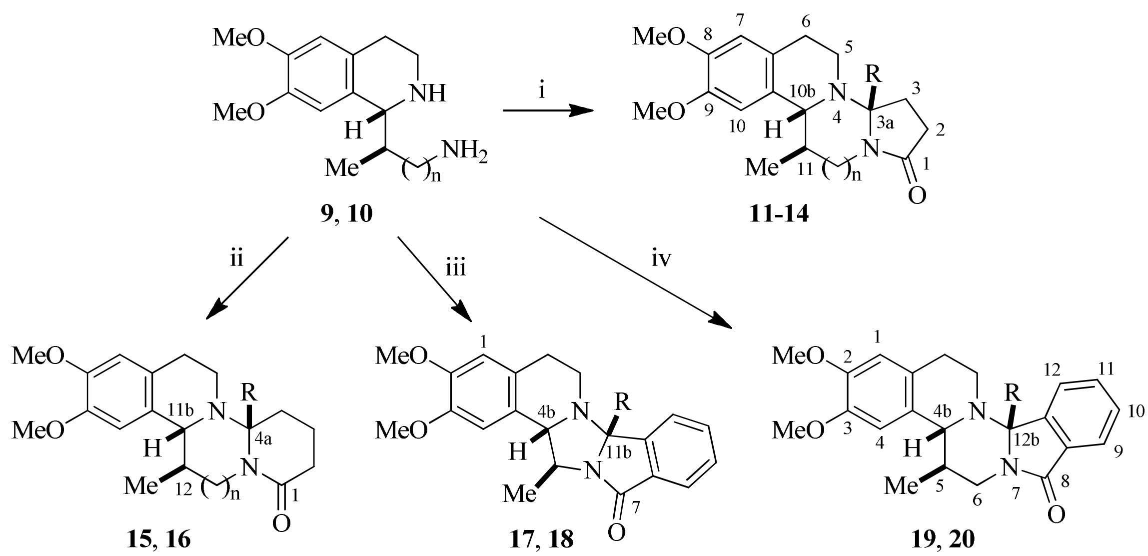

	9	10	11	12	13	14	15	16	17	18	19	20
n	0	1	0	0	1	1	0	1	–	–	–	–
R	–	–	Me	Ph	Me	Ph	Ph	Ph	H	Ph	H	Ph

Scheme 3. *Reagents and conditions:* (i) $RCO(CH_2)_2COOH$, toluene, reflux, 4-8 h, 59-77%; (ii) $PhCO(CH_2)_3COOH$, toluene, reflux, 10-12 h, 52-63%; (iii) 2-RCO-C_6H_4COOH, toluene, reflux, 2-3 h, 63-74%; (iv) 2-RCO-C_6H_4COOH, toluene, reflux, 2-3 h, 58-76%.

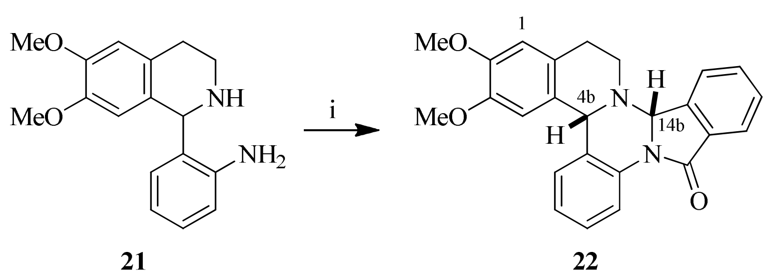

Scheme 4. *Reagents and conditions:* (i) 2-HCO-C_6H_4COOH, toluene, PTSA, reflux, 12 h, 62%.

NMR spectroscopic structure determination

The solution structures of products **11–20** and **22** were determined by ^{1}H and ^{13}C NMR spectroscopy in $CDCl_3$ solution. The ^{1}H and ^{13}C chemical shifts of these compounds were assigned with the help of standard 2D NMR correlation spectra (dqf-COSY, NOESY, multiplicity-edited HSQC and HMBC). The stereo assignment of diastereotopic protons, and the analysis of relative configuration and conformation was based on NOEs and $J_{H,H}$-coupling constant values. Accurate ^{1}H chemical shifts and $J_{H,H}$-coupling constants were obtained from computer simulation and iteration of the 1D ^{1}H NMR spectra. The NMR data are presented in

Tables 1–3. Below, the diastereotopic hydrogens which are on the same side of the polycycle as the isoquinoline bridgehead hydrogen will be labelled as *syn* or *s*, and as *anti* or *a* otherwise. Compounds **11–14** contain three asymmetric carbons (C3a, C10b, C11), as do **15–16** (C4a, C11b, C12), **17–18** (C4b, C5, C11b) and **19–20** (C4b, C5, C12b), whereas **22** contains two (C4b, C14b). Of these, the R-bearing carbon atom (C3a for **11** etc.) is a new stereo centre formed during the domino ring-closure and its configuration is, a priori, unknown. The syntheses were highly stereo-selective, so that only one of the two possible epimers was produced to a notable extent. For each product, proton–proton NOE correlations proved that the relative positions of the substituents carried by the three asymmetric carbons (two for **22**) is all-*cis*, as shown in Schemes 2 and 3. These NOEs also verify the configuration of the starting diamines **9** and **10**.

Table 1. Proton chemical shifts δ_H (in ppm, $CDCl_3$, 298 K) of **11–22**. The label *s* (*a*) indicates that the hydrogen is *syn* (*anti*) with respect to the isoquinoline bridgehead hydrogen. The chemical shifts marked with an asterisk (*) may be interchanged

	11	**12**	**13**	**14**		**15**	**16**
R	Me	Ph	Me	Ph	R	Ph	Ph
n	0	0	1	1	n	0	1
2*s*	2.81	2.82	2.49	2.52	2*s*	2.57	2.50
2*a*	2.45	2.51	2.50	2.58	2*a*	2.39	2.52
					3*s*	1.52	1.49
					3*a*	1.70	1.68
3*s*	2.02	2.05	2.08	1.98	4*s*	1.99	1.77
3*a*	2.17	2.73	2.33	2.49	4*a*	2.15	2.51
5*s*	2.69	3.18	2.88	3.20	6*s*	3.32	3.59
5*a*	2.95	2.50	2.95	3.13	6*a*	2.65	3.22
6*s*	2.82	3.09	2.90	3.15	7*s*	3.09	3.12
6*a*	3.01	2.81	2.82	2.85	7*a*	2.80	2.88
7	6.63*	6.63	6.60	6.65	8	6.62	6.65
8-OMe	3.84	3.84	3.84	3.86	9-OMe	3.84	3.86
9-OMe	3.84	3.76	3.84	3.75	10-OMe	3.75	3.75
10	6.62*	6.44	6.59	6.31	11	6.46	6.30
10b	3.86	3.77	4.06	3.62	11b	3.50	3.48
11*a*	3.91	3.80	2.01	2.12	12*a*	3.95	2.16
11-Me	1.61	1.46	1.02	0.78	12-Me	1.54	0.77
12*s*	-	-	2.76	2.70	13*s*	-	2.55
12*a*	-	-	4.10	4.19	13*a*	-	4.66
R	1.42	7.62 *o*	1.67	7.49 *o*	R	7.54 *o*	7.1(br) *o*
		7.36 *m*		7.38 *m*		7.35 *m*	7.6(br) *o′*
		7.30 *p*		7.30 *p*		7.30 *p*	7.36 *m*
							7.29 *p*

Table 1. (Continued)

	17	**18**		**19**	**20**		**22**
R	H	Ph	R	H	Ph	R	H
n	0	0	n	1	1	n	-
1	6.60	6.62	1	6.60	6.62	1	6.65
2-OMe	3.84	3.84	2-OMe	3.85	3.85	2-OMe	3.86
3-OMe	3.88	3.79	3-OMe	3.87	3.79	3-OMe	3.98
4	6.67	6.51	4	6.62	6.42	4	6.89
4b	4.18	4.12	4b	3.85	3.79	4b	5.51
5*a*	3.85	3.96	5*a*	2.19	2.20	5	7.28
5-Me	1.69	1.55	5-Me	1.05	0.88	6	7.05
			6*s*	2.96	2.85	7	7.33
			6*a*	4.45	4.49	8	8.71
8	7.83	7.81	9	7.87	7.87	11	7.96
9	7.54	7.44	10	7.53	7.40	12	7.60
10	7.61	7.46	11	7.58	7.43	13	7.67
11	7.63	7.23	12	7.60	7.21	14	7.71
13*s*	2.39	2.49	14*s*	2.38	2.54	16*s*	2.32
13*a*	2.18	2.08	14*a*	2.78	2.88	16*a*	2.44
14*s*	2.90	3.04	15*s*	2.89	3.00	17*s*	2.91
14*a*	2.60	2.57	15*a*	2.63	2.64	17*a*	2.56
R	5.65	7.80 *o*	R	5.58	7.2(br) *o*	R	6.08
		7.35 *m*			8.1(br) *o′*		
		7.30 *p*			7.36(br) *m*		
					7.29 *p*		

The preferred conformations of the polycyclic products could be deduced from the *J*-coupling constants and NOE correlations between protons, and by using the structural information thus obtained as constraints in molecular mechanics modelling. Compound **11** showed an NOE correlation between all pairs of 3a-Me, 5-H_{syn} and 10b-H, indicating their mutual spatial proximity, and also displayed large $^3J_{H,H}(5s,6a)$ and $^3J_{H,H}(10b,11a)$ coupling values implying these hydrogens to be antiperiplanar. On the other hand, the 5-H_{syn} proton of **12–14**, and the analogous proton of derivatives **15–20** and **22** (6-H_{syn} of **15** etc.), typically did not share an NOE correlation with the substituent R or the isoquinoline bridgehead proton. Instead, these derivatives showed an NOE between 5-H_{anti} and 11-H_{anti} (**12–14**), 6-H_{anti} and 12-H_{anti} (**15–16**) etc. The derivatives **12–20** and **22** also had large $^3J_{H,H}(5a,6s)$ (**12–14**), $^3J_{H,H}(6a,7s)$ (**15–16**) etc. values (as opposed to large $^3J_{H,H}(5s,6a)$ etc.). These data suggest two conformations populated by these compounds: **11** prefers a conformation in which the ring B (tetrahydropyridine) is approximately *trans*-fused with the ring C (imidazolidine) whilst the other derivatives prefer a *cis*-fused conformation between rings B and C (the latter being either imidazolidine, n = 0, or hexahydropyrimidine, n = 1). Ring B adopts a half-chair conformation with the two aromatic carbons and the aliphatic carbons attached to them defining a plane, and the remaining methylene carbon (C5 etc.) and nitrogen (N4 etc.) lying above and below this plane. In **11,** it is the methylene carbon (C5) which lies on the same side of the plane as the bridgehead hydrogen (10b-H), whereas in **12–20** and **22** the *syn* atom is nitrogen (**12–14**: N4, **15–16**: N5, **17–18**: N12, **19–20**: N13, **22**: N15). These *trans*-B/C and *cis*-B/C conformations are depicted in Figures 1 and 2 for **11** and **16**, respectively.

There is a possibility for an equilibrium between the *trans*-B/C and *cis*-B/C conformers, involving the ring inversion of ring B combined with an umbrella inversion of its nitrogen atom. In a pure *trans*-B/C conformation, $^3J_{H,H}$(5*s*,6*a*) (**11–14**) or the analogous coupling (**15–20**, **22**) would be large while the corresponding $^3J_{H,H}$(5*a*,6*s*) etc. coupling would be small. In the *cis*-B/C conformation, the opposite would be true. In case of a fast equilibrium, the observed values of these coupling constants become population-weighted averages of the “large” (ca. 12.2 Hz) and

Table 2. Proton–proton coupling constants $J_{H,H}$ (in Hz, $CDCl_3$, 298 K) of **11–22**. The label *s* (*a*) indicates that the hydrogen is *syn* (*anti*) with respect to the bridgehead hydrogen

	11	**12**	**13**	**14**		**15**	**16**
R	Me	Ph	Me	Ph	R	Ph	Ph
n	0	0	1	1	n	0	1
2*s*,2*a*	-17.0	-17.2	-17.5	-17.6	2*s*,2*a*	-18.4	-18.2
2*s*,3*s*	9.6	10.3	10.4	10.6	2*s*,3*s*	6.6	5.1
2*s*,3*a*	10.3	7.5	4.5	2.8	2*s*,3*a*	1.5	4.6
2*a*,3*s*	2.4	4.5	7.3	8.9	2*a*,3*s*	11.4	10.1
2*a*,3*a*	10.2	10.4	10.3	10.1	2*a*,3*a*	7.8	6.2
3*s*,3*a*	-12.7	-14.1	-14.2	-14.8	3*s*,3*a*	-12.8	-13.7
					3*s*,4*s*	3.0	2.9
					3*s*,4*a*	13.4	10.9
					3*a*,4*s*	4.0	6.6
					3*a*,4*a*	3.3	3.3
					4*s*,4*a*	-12.5	-13.6
5*s*,5*a*	-10.8	-10.2	-11.5	-11.3	6*s*,6*a*	-10.3	-11.7
5*s*,6*s*	5.0	5.3	6.7	7.5	6*s*,7*s*	5.5	7.6
5*s*,6*a*	10.3	2.8	3.3	1.3	6*s*,7*a*	2.5	1.8
5*a*,6*s*	2.5	11.2	9.9	11.6	6*a*,7*s*	11.7	10.8
5*a*,6*a*	7.0	3.8	5.1	4.9	6*a*,7*a*	3.7	5.2
6*s*,6*a*	-16.4	-16.0	-16.3	-16.4	7*s*,7*a*	-16.1	-16.5
10b,11*a*	8.2	9.7	10.6	10.8	11b,12*a*	9.5	10.8
11*a*,11-Me	6.3	6.3	6.6	6.5	12*a*,12-Me	6.1	6.5
11*a*,12*s*	-	-	11.9	11.8	12*a*,13*s*	-	12.0
11*a*,12*a*	-	-	5.3	5.2	12*a*,13*a*	-	5.0
12*s*,12*a*	-	-	-13.5	-13.3	13*s*,13*a*	-	-13.7

Table 2. (Continued)

	17	**18**		**19**	**20**		**22**
R	H	Ph	R	H	Ph	R	H
n	0	0	n	1	1	n	-
4b,5*a*	8.6	8.7	4b,5*a*	10.3	10.7	5,6	7.8
5*a*,5-Me	6.2	6.3	5*a*,5-Me	6.6	6.6	5,7	1.3
			5*a*,6*s*	11.5	11.7	6,7	7.4
			5*a*,6*a*	5.3	5.2	6,8	1.3
			6*s*,6*a*	-13.4	-13.4	7,8	8.2
8,9	7.6	7.6	9,10	7.6	7.6	11,12	7.6
8,10	1.1	1.2	9,11	1.1	1.1	11,13	1.1
9,10	7.5	7.4	10,11	7.5	7.4	12,13	7.4
9,11	1.0	1.0	10,12	1.0	1.0	12,14	0.9
10,11	7.6	7.6	11,12	7.5	7.6	13,14	7.6
13*s*,13*a*	-11.0	-10.9	14*s*,14*a*	-12.0	-11.9	16*s*,16*a*	-11.6
13*s*,14*s*	5.6	5.4	14*s*,15*s*	7.8	7.7	16*s*,17*s*	6.9
13*s*,14*a*	3.3	1.9	14*s*,15*a*	1.0	1.5	16*s*,17*a*	1.4
13*a*,14*s*	10.5	12.2	14*a*,15*s*	11.4	11.3	16*a*,17*s*	11.8
13*a*,14*a*	4.2	3.4	14*a*,15*a*	5.3	5.0	16*a*,17*a*	4.7
14*s*,14*a*	-16.3	-16.1	15*s*,15*a*	-16.6	-16.5	17*s*,17*a*	-16.4

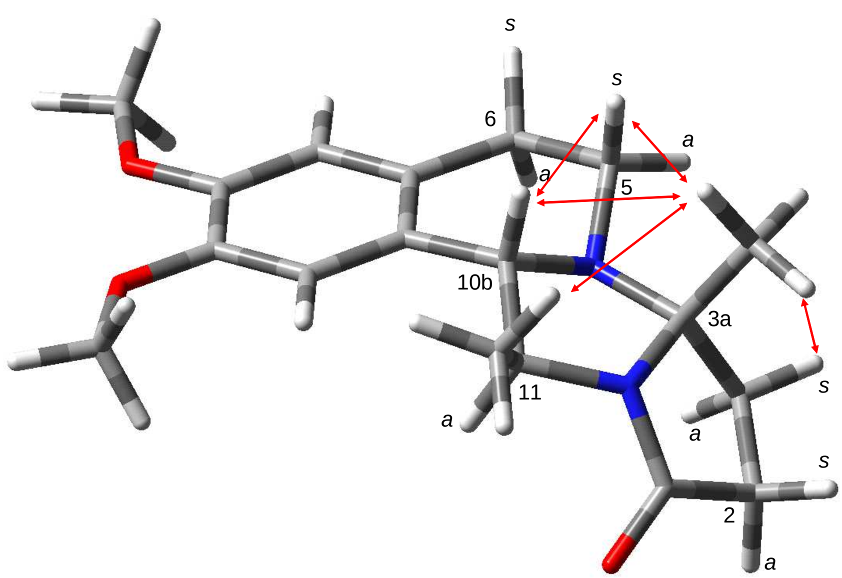

Figure 1. The preferred conformation, *trans*-B/C, of **11** in $CDCl_3$ solution at 298 K as obtained from MM optimization with constraints from NMR spectroscopic analysis. Relevant NOE correlations are indicated with double-headed arrows.

"small" (ca. 1 Hz) limiting value. Using the *J*-data from Table 2 this allows for a rough estimate: **11** is ca. 85% *trans*-B/C, **13** and **17** are 80–85% *cis*-B/C and the rest are 90–100% *cis*-B/C. Thus, increasing the size of the substituent R or adding a condensed benzene ring (ring E) on the lactam ring seems to shift the equilibrium towards the *cis*-fused conformation. This is consistent with our previous findings on similar structures which lack the methyl substituent at ring C.[5] Comparing the results, this methyl substitution in itself seems to cause a shift towards the *cis*-B/C conformation.

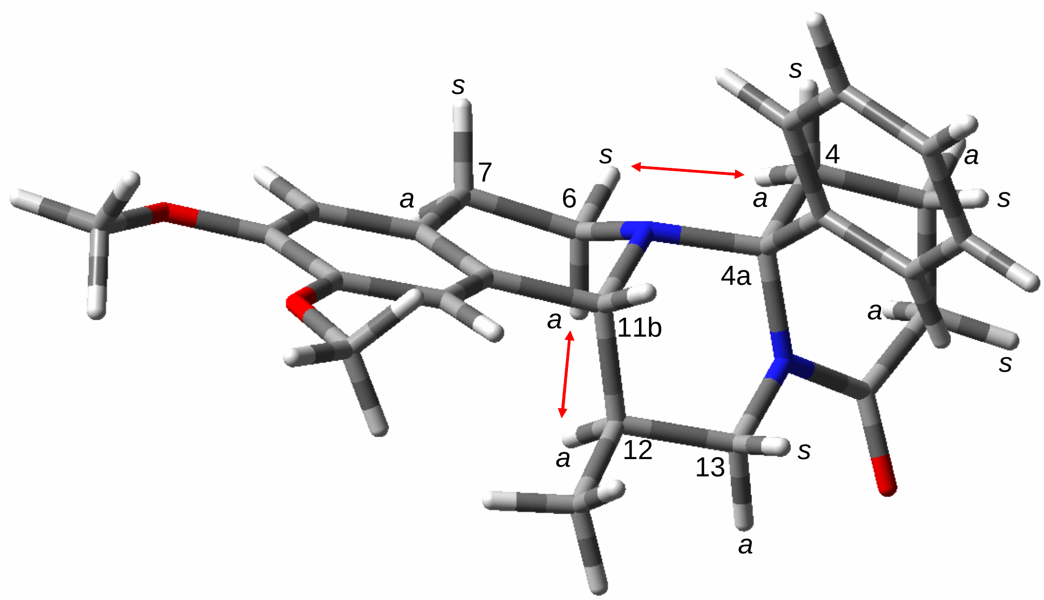

Figure 2. The preferred conformation, *cis*-B/C, of **16** in $CDCl_3$ solution at 298 K as obtained from MM optimization with constraints from NMR spectroscopic analysis. Relevant NOE correlations are indicated with double-headed arrows.

The terminal six-membered piperidine ring in **15** and **16** (ring D) displayed large vicinal H,H-coupling constants within the *anti*–*syn*–*anti* sequence of its protons (i.e. $^3J_{H,H}(2a,3s)$ and $^3J_{H,H}(3s,4a)$), implying their *trans*-diaxial relationship. This is consistent with a chair or half-chair (with the amide group close to planar) conformation, with R in a (pseudo)axial position. When the terminal ring D is five-membered (pyrrolidine; derivatives **11**–**14**) the *J*-coupling between the *syn* protons (2*s*,3*s*) is large, as is the coupling between the *anti* protons (2*a*,3*a*). Therefore, in the preferred conformation of this ring the *syn* hydrogens nearly eclipse each other (as do the *anti* hydrogens). For **11** and **12** (**13** and **14**), the eclipsed conformation is slightly opened so that the 2*s* and 3*a* (2*a* and 3*s*) hydrogens become more antiperiplanar. The *ortho* protons of the phenyl group in phenyl-substituted (R = Ph) derivatives **16** and **20** were nonequivalent and heavily broadened at 298 K, indicating that the rotation of this substituent is restricted and takes place in the slow–intermediate NMR time scale. The other phenyl-substituted compounds (**12**, **14**, **15**, **18**) did not show similar signal splitting. Apparently, there are steric 1,3-diaxial interactions present when the rings C and/or D are six-membered (hexahydropyrimidine and piperidine, respectively), which in case of **16** and **20** slow down the rotation of the phenyl substituent sufficiently to cause the observed ^{1}H signal splitting of the *ortho* protons.

Table 3. Carbon chemical shifts δ_C (in ppm, $CDCl_3$, 298 K) of **11–22**. The assignment between shifts marked with a similar symbol is uncertain

	11	**12**	**13**	**14**		**15**	**16**
R	Me	Ph	Me	Ph	R	Ph	Ph
n	0	0	1	1	n	0	1
1	176.7	177.6	172.4	174.4	1	169.9	171.9
2	33.3	32.9	30.2	30.2	2	31.5	33.0
					3	16.4	17.3
3	33.3	30.1	31.3	33.0	4	32.3	36.6
3a	83.9	92.0	78.3	84.4	4a	87.4	81.6
5	42.0	41.0	38.8	37.6	6	41.4	37.6
6	29.1	28.9	29.0	28.8	7	28.9	28.9
6a	126.0$^{\#}$	125.8*	126.6†	126.1	7a	125.7*	126.3
7	111.9	111.2	111.4	111.3	8	111.1	111.2
8	148.0*	148.0	148.1	148.1	9	148.0	148.0
8-OMe	56.0†	55.8	55.8*	55.8	9-OMe	55.8	55.8
9	147.3*	147.3	146.1	145.9	10	147.2	145.9
9-OMe	55.9†	55.9	56.1*	56.0	10-OMe	55.8	56.0
10	107.4	109.2	112.3	112.0	11	109.6	112.0
10a	128.2$^{\#}$	125.6*	127.7†	127.8	11a	125.7*	128.2
10b	69.1	68.8	60.2	60.7	11b	63.7	60.1
11	55.1	55.5	29.9	28.0	12	57.0	29.1
11-Me	22.4	19.1	17.1	16.7	12-Me	18.0	16.9
12	-	-	42.9	43.9	13	-	45.3
R	19.6	*i* 145.3	23.4	144.5	R	144.5	144.2
		o 125.5		125.7		127.2	129(br)
		m 128.4		129.2		127.8	127.0
		p 127.6		127.4		127.6	127.3

Table 3. (Continued)

	17	18		19	20		22
R	H	Ph	R	H	Ph	R	H
n	0	0	n	1	1	n	-
1	111.5	111.3	1	111.7	111.4	1	112.0
2	148.2	148.1	2	148.4	148.2	2	148.6
2-OMe	55.8	55.9	2-OMe	55.8	55.8	2-OMe	55.9
3	147.3	147.3	3	146.2	145.9	3	146.8
3-OMe	56.0	55.9	3-OMe	56.2	56.0	3-OMe	56.3
4	108.9	109.3	4	112.2	112.2	4	113.1
4a	125.6	125.9	4a	127.4	127.7	4a	126.3
4b	73.1	70.9	4b	65.2	60.2	4b	61.5
5	54.5	55.3	5	27.9	28.1	4c	124.3
5-Me	20.4	20.0	5-Me	16.8	16.7	5	128.0
			6	45.6	43.2	6	124.0
						7	128.0
						8	118.7
						8a	140.2
7	171.4	172.4	8	165.3	166.6	10	165.8
7a	135.6	133.1	8a	133.8	131.0	10a	133.6*
8	124.3	124.3	9	123.9	124.1	11	124.0
9	129.8	129.3	10	129.4	128.7	12	129.9
10	132.1	132.4	11	131.7	132.0	13	132.6
11	124.3	124.3	12	123.3	123.2	14	123.2
11a	140.5	145.8	12a	140.8	147.5	14a	135.2*
11b	81.8	93.6	12b	76.5	84.5	14b	77.3
13	41.3	42.8	14	36.4	38.6	16	37.4
14	28.3	28.8	15	27.9	28.5	17	27.9
14a	125.8	125.9	15a	126.1	126.3	17a	126.5
R	-	*i* 141.3	R	-	139.6	R	-
		o 125.9			126.1(br)		
		m 128.7			129.4		
		p 128.2			128.1		

Mass spectrometric fragmentations

The primary fragmentations of compounds **11-20** and **22** are based on ring cleavages occurring in ring C (Scheme 5 and Table 4). The substitution (H, Me or Ph) at the position 3a (**11–14**), 4a (**15** and **16**), 11b (**17**, **18**), 12b (**19**, **20**) or 14b (**22**) as well as n = 0 or 1 (Scheme 3) seems to have fairly decisive effect on the type of fragments obtained. For all compounds, ring C splits into relatively strong ion **a+1** which is even the base peak when n = 1 and R = Me or Ph and into [**M–a**]$^{+\bullet}$ which in turn is the base peak when n = 0 and R = H or Ph (**17** and **18).** Furthermore, **11**, **16**, **19**, **20** and **22** give some amount of the ion **a–1** which is the base peak for **19** (n = 1 and

R = Ph). The complementary ion [M–**a**]$^{+\bullet}$ is the base peak for **17** and **18** (n = 0 and R = H or Ph) and also rather strong for the other compounds except **11** and **22**. All compounds except **11**, **13**, **17** (n = 0, 1, 0 and R = Me, Me and H, respectively) and **22** (H at C-14b) give relatively strong complementary ion [M–(**a+1**)]$^+$ which is even the base peak for **14** and **20** (n = 1 and R = Ph). Compounds **14**, **19** and **20** (n = 1; R = Ph, H, Ph, respectively) give also a weak ion [M–(**a–1**)]$^+$ and compounds **12**, **14**, and **15** (n = 0, 1 and 0, respectively and R = Ph) a weak ion [M–(**a+2**)]$^{+\bullet}$. Ring C additionally splits into ion **b**, which contains the CH_3CH-group (Scheme 5) more than ion **a**. Ion **b** is the base peak for **12** (n = 0 and R = Ph) and abundant for **15** (n = 0 and R = Ph) and present also in the spectra of **17** and **18** (n = 0, R = H and Ph). It is interesting that compounds **11**, **15** and **19** (n = 0 and 1; R = Me, Ph and H, respectively) give the ion **b–1** of which, however, only **15** (n = 0, R = Ph) exhibited also the ion **b**.

Table 4. Main fragments [*m/*z(RA %)] from the studied compounds under electron ionization. **b**: $C_{13}H_{17}NO_2^{+\bullet}$, (**b–1**): $C_{13}H_{16}NO_2^+$, (**a+1**): $C_{11}H_{14}NO_2^+$, **a**: $C_{11}H_{13}NO_2^{+\bullet}$, (**a–1**): $C_{11}H_{12}NO_2^+$. The base peaks are written in italics

Cmpd	$M^{+\bullet}$	[M–H]$^+$	[M–CH_3]$^+$	**b**	(**b–1**)	(**a+1**)	**a** (**a–1**)
11[a]	316(6)	315(31)[b]		219(16)	218(39)	*192(100)*[c]	191(3) 190(15)
12	378(1)	377(1)	[M–Ph]$^+$ 301(6)	*219(100)*	-	192(22)	- -
13	330(3)	329(0.4)	[M–CH_3]$^+$ 315(17)	-	-	*192(100)*	191(5.5) -
14	392(2)	-	[M–Ph]$^+$ 315(3)	-	-	192(82)	- -
15	392(62)	391(11)	*315(100)*	219(82)	218(4)	192(38)	- -
16	406(14)	405(0.9)	[M–Ph]$^+$ 329(8.5)	-	-	*192(100)*	191(11) 190(6)
17	350(17)	349(1)	-	219(8)	-	192(40)	- -
18	426(24)	425(0.7)	-	219(33)[d]	-	192(38)	191(5) -
19	364(26)	363(3)	-	-	$C_{13}H_{17}NO_2^+$ 218(7)	192(9)	191(7) *190(100)*
20	440(2)	439(0.4)	-	-	-	192(86)	191(5) 190(9)
22	398(72.5)	*397(100)*	[M–CH_3]$^+$ 383(8)	-[e]	-	192(20)	191(2) 190(21)

[a]MS/MS 20.42–24.96 eV. [b]In fact [M+H–H_2]$^+$. [c]Also **a**+**2**: 193(17). [d](**b+1**) 220(7). [e](**b+1**) 220(10).

Table 4. (Continued)

Cmpd	$C_{13}H_9^+$	*m/z 176*	$[M–\mathbf{a}]^{+\bullet}$	$[M–(\mathbf{a}+1)]^+$	$[M–(\mathbf{a}–1)]^+$	$[M–(\mathbf{a}+2)]^{+\bullet}$
11	-	$[(\mathbf{b}–1)–C_3H_6]^+$ (94)	$C_7H_{12}NO^{+\bullet}$ 126(35)	-	[f]-	-
12	-	$[\mathbf{b}–C_3H_7]^+$, $[\mathbf{a}–CH_3]^+$ (3)	$C_{12}H_{13}NO^{+\bullet}$ 187(44)	$C_{12}H_{12}NO^+$ 186(52)	-	$C_{12}H_{11}NO^{+\bullet}$ 185(9)
13	-	-	$C_8H_{13}NO^{+\bullet}$ 139(18)	-	-	-
14	-	$[\mathbf{a}–CH_3]^+$ (5)	$C_{13}H_{14}NO^+$ 201(47)	$C_{13}H_{14}NO^+$ *200(100)*	$C_{13}H_{16}NO^+$ 202(8)	$C_{13}H_{13}NO^{+\bullet}$ 199(9.5)
15	-	$[\mathbf{b}–C_3H_7]^+$, $[\mathbf{a}–CH_3]^+$ (6)	$C_{13}H_{15}NO^{+\bullet}$ 201(29)	$C_{13}H_{14}NO^+$ 200(68)	-	$C_{13}H_{13}NO^{+\bullet}$ 199(7)
16	-	$[(\mathbf{b}–1)–C_3H_6]^+$ (10)	$C_{14}H_{17}NO^{+\bullet}$ 215(56)	$C_{14}H_{16}NO^+$ 214(79)	-	-
17	-	-	$C_{10}H_9NO^{+\bullet}$ *159(100)*	-	-	-
18	165(28)	-	$C_{16}H_{13}NO^{+\bullet}$ *235(100)*	$C_{16}H_{12}NO^+$ 234(65)	-	-
19	-	$[(\mathbf{b}–1)–C_3H_6]^+$ (8)	$C_{11}H_{11}NO^{+\bullet}$ 173(74)	$C_{11}H_{10}NO^+$ 172(5)	$C_{11}H_{12}NO^+$ 174(8)[g,h]	-
20	165(16.5)	$[(\mathbf{b}–1)–C_3H_6]^+$ (7)	$C_{17}H_{15}NO^{+\bullet}$ 249(80)	$C_{17}H_{14}NO^+$ *248(100)*	-	-
22	165(30)	-	$C_{14}H_9NO^{+\bullet}$ 207(5)	-	$C_{14}H_{10}NO^+$ 208(19)	-

[f]Gives also the ion $C_{11}H_{12}NO^+$:174(13). [g]Contains 1/9 of $C_{10}H_8NO_2^+$. [h]$[M–(\mathbf{a}–2)]^{+\bullet}$: $C_{11}H_{13}NO^{+\bullet}$ 175(6); contains 1/6 of $C_{10}H_9NO_2^{+\bullet}$.

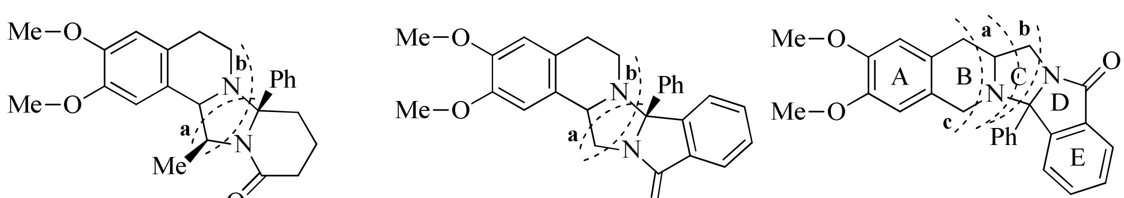

15 **I** **II**

Scheme 5. The primary fragmentation routes for linearly-condensed compounds (**15** as an example) studied in this work in comparison with the major fragmentations (**I** and **II**) of the polycyclic lactams reported earlier. [5b]

All compounds except **13**, **17**, **18** and **22** give also some amount of the ion *m/z* 176 which for **11**, **16**, **18** and **20** (n = 0, 1, 0 and 1; R = Me, Ph, Ph and Ph, respectively) corresponds to $[(\mathbf{b}–1)–C_3H_6]^+$ whereas **12** and **15** (n = 0 and R = Ph) exhibiting a strong ion **b**, give the ion [**b**–C_3H_7]$^+$ or [M–**a**–CH_3]$^+$ instead. For **14** (n = 1, R = Ph) *m/z* 176 corresponds to ion [**a**–CH_3]$^+$. For **11** and **15** for which n = 0 and R = Me or Ph (Scheme 3), [M–CH_3]$^+$ is the base peak and also **13** (n = 1, R = Me) and **22** (H at C-4b) give a small amount of [M–CH_3]$^+$ ion whereas **12** (n = 0, R = Ph), **14** (n = 1, R = Ph) and **16** (n = 1, R = Ph) give a fairly weak ion [M–Ph]$^+$ instead.

The hexacyclic lactam is greatly stabilized by the benzo-fusions which is proved by the fact that its base peak is [M–H]$^+$ and also the molecular ion is very strong (72%). This is on line with the observation that otherwise it gives a great number of medium or weak ions (Tables 4 and 5). As to the other compounds **11**, **13**, **14**, **17** and **18** give relatively few and mainly low mass fragments whereas compounds **12**, **15**, **16**, **19**, and **20** give rather many further fragments (Table 5). The common features for the first-mentioned group seem to be that n = 0 (**11**, **17** and **18**) or n = 1 and R = Me or Ph (**13** and **14**). As to the second group the common features are n = 0 or 1 and R = Ph (**12**, **15**, **16** and **20**), for **19** n = 1 and R = H. If we compare this situation with the groups in Scheme 1 **12**, **17** and **18** (n = 0 and R = Ph) fall out from these groups probably due to the five-membered ring in **12** and the benzo-fusion (and n = 1) in **17** and **18**. On the other hand **15**, **16**, **19** and **20** consist of a six-membered oxo-ring + R=Ph (**15** and **16**) and a benzo-fusion with n = 1 (**19** and **20**).

Table 5. Other ions *(m/z* [RA≈5%])

Cmpd	
11	[M+H–**b**]$^{+\bullet}$=$C_5H_8NO^{+\bullet}$: 98(14)[a]
12	$C_{11}H_{13}N^{+\bullet}$: 159(8); $C_{11}H_{12}N^+$: 158(5); $C_{10}H_{10}N^+$: 144(12); $C_9H_9N^{+\bullet}$: 131(21); $C_9H_8N^+$: 130(7); $C_8H_7N^{+\bullet}$+$C_9H_9^+$ (1:1): 117(8); $C_7H_6N^+$+$C_8H_8^{+\bullet}$ (6:1): 104(10); $C_7H_5N^{+\bullet}$+$C_8H_7^+$ (1:1): 103(11); 56(5)
13	$C_7H_{10}N^+$: 124(21); $C_6H_9NO^{+\bullet}$: 111(22.5); $C_5H_8NO^+$: 98(41); 55(6), 56(6), 42(7)
14	$C_{10}H_{10}NO^+$: 160(9.5); $C_{11}H_{12}N^+$: 158(6); 117(7); $C_7H_6N^+$: 104(6); 103(5); 56(6)
15	[M–C_2H_5]$^+$: 363(19); [M–C_4H_7O]$^+$: 321(13); [M–C_7H_9]$^+$: 299(11); [M–C_5H_8NO]$^+$: 294(30); $C_{12}H_{14}N^+$: 172(25); $C_{11}H_{12}N^+$: 158(27.5); $C_9H_9N^{+\bullet}$: 131(16); $C_9H_8N^+$: 130(10); 104(14); 103(20); 91(5); 77(7), 55(12)
16	[M–C_7H_7]$^+$: 315(11); $C_{13}H_{14}NO^+$: 200(12); 186(5), 174(5); 145(29), 130(8), 117(8), 103(7); 69(6); 58(7); 55(6.5); 43(19); 42(7)
17	130(21); 90(18)
18	$C_{15}H_{12}N^+$: 206(16); 58(5); 43(15)
19	$C_{10}H_8NO^+$: 158(12); 146(6); 145(4); 144(5); $C_8H_6NO^+$: 132(29); 130(6); $C_8H_7N^{+\bullet}$: 117(11); $C_7H_4O^{+\bullet}$+$C_7H_6N^+$ (3:1): 104(13); 103(5); 90(5); 77(5); 43(10); 41(6)
20	$C_{16}H_{12}NO^+$: 234(6); $C_{16}H_{14}N^+$+$C_{15}H_{10}NO^+$ (3:1): 220(14); $C_{14}H_{10}NO^+$: 208(8); $C_{14}H_8NO^+$+$C_{15}H_{12}N^+$ (4:1): 206(8); $C_{13}H_9N^{+\bullet}$: 179(6); 130(8); 104(6); 58(10); 43(33)
22	([M–C_2H_5]$^+$+[M–CHO]$^+$): 369(20); 301(10); $C_{16}H_{12}N_2O^{+\bullet}$: 248(5); $C_{16}H_{11}N_2O^+$: 247(5); $C_{15}H_9N_2O_3^+$: 233(12); $C_{12}H_{12}NO^+$: 186(24); $C_{10}H_{13}NO_2^{+\bullet}$+$C_{13}H_9N^{+\bullet}$ (1:1): 179(17); $C_{10}H_{12}NO_2^+$+$C_{13}H_8N^+$ (2:5): 178(8); 77(12); 69(5); 57(7); 44(14); 43(7); 41(6); 40(11)

[a]MS/MS from [M+H]$^+$ at 33.57–41.03 eV. For the other results at this voltage see Experimental, compound **11**.

Conclusions

Our results demonstrate that 1-substituted 1,2,3,4-tetrahydroisoquinoline 1,2- and 1,3-diamines, bearing a methyl substituent or an aromatic ring in the side chain, were conveniently transformed to tetra-, penta- and hexacyclic lactams by domino cyclocondensations with acyclic or aromatic γ- or δ-oxo acids. The NMR analyses proved that each cyclocondensations took place with practically full diastereoselectivity (*de* ~100%) in favour of the *cis* isomer. Compound **11** prefers a conformation with a *trans*-B/C ring fusion, whereas the other derivatives (**12–20**, **22**) favour *cis*-B/C fusion. These conformers can change into each other through a ring-inversion of ring B combined with an umbrella inversion of its nitrogen atom, but the population of the preferred conformer is always 80–100%. Increasing the size of substituent R, or adding a condensed benzene ring at the lactam ring, shifts the conformational equilibrium towards the *cis*-B/C conformer.

Experimental Section

General. Melting points were measured on a Kofler hot-plate microscope apparatus and are uncorrected. Column chromatography was performed with silica gel 60 (0.063-0.200). For routine thin-layer chromatography (TLC), Silica gel 60 F_{254} plates (Merck, Germany) were used. Elemental analyses were performed with a Perkin-Elmer 2400 CHNS elemental analyser. Compounds **10**[7] and **21**[8] were prepared according to known procedures.

NMR spectra

The NMR spectra were recorded in $CDCl_3$, DMSO-d_6 or D_2O solutions on JEOL JNM-LA400, Bruker AVANCE DRX 400 and AVANCE 500 spectrometers. Chemical shifts are given in δ (ppm) relative to TMS ($CDCl_3$ and DMSO-d_6) or to TSP (D_2O) as internal standards. The spectra of the products were acquired without sample spinning at 298 K. The NMR experiments consisted of standard ^{1}H NMR (using a 30º flip angle and a 5 s pulse repetition time), ^{13}C NMR with broad-band proton decoupling, dqf-COSY, 1D and 2D NOESY (with a mixing time of 0.3 s), multiplicity-edited HSQC (optimized for a one-bond coupling of 145 Hz and set to show CH and CH_3 signals positive and CH_2 signals negative), and HMBC (optimized for long-range couplings of 8 Hz with a low-pass *J*-filter optimized to remove signals due to one-bond coupling around 145 Hz) measurements. Proton chemical shifts δ_H and proton–proton coupling constants $J_{H,H}$ were extracted by using the spectral simulation and analysis tool PER included in the PERCH NMR software package (version 2008.1).[12] The initial guess for the NMR parameters was obtained manually from the ^{1}H spectra or by trial-and-error in case of crowded/complicated spectral regions, which was then refined iteratively by using the integral-transform and total line-shape-fitting modes of the software. Manual adjustment and iterative fitting of parameters was repeated until good visual comparison was achieved between the calculated and the observed spectra. Structural models were obtained from molecular-mechanics modelling (MM+ force field) by using the HyperChem 7.0 software. Distance and torsion angle restraints (with the software's default force constants) were applied in the initial modelling based on the observed NOE and *J*-coupling constant data, and when a satisfactory structure was obtained it was refined without restraints to yield the final model.

Mass spectral measurements

The electron ionization mass spectra (Tables 4 and 5) were recorded on a VG ZABSpec mass spectrometer (VG Analytical, Division of Fisons, Manchester, UK) equipped with the Opus V3.3X program package (Fisons Instruments, Manchester, UK). The ionization energy used was 70 eV and the source temperature was 160 °C. The accelerating voltage was 8 kV and the trap current was 200 mA. Perfluorokerosene was used to calibrate the mass scale. A small amount of solid sample dissolved in MeOH was placed in a capillary tube and the solvent was evaporated off with hot air. Thereafter, the sample was introduced into the ionization chamber via the solid inlet. The fragmentation pathways were confirmed by linked scans at constant B/E or B^2/E (first field-free region, FFR1) without collision gas. The low-resolution B/E and B^2/E spectra were measured with a resolving power of 3000 (10% valley definition). The accurate masses were determined by voltage scanning with a resolving power of 6000-10,000. The compositions of the molecular ions based on their accurate masses are given in Table 6.

For the low-resolution spectra, consecutive scans selected from the stable and constant part of the total ion current chromatogram were averaged to obtain more reproducible abundances. For accurate masses and linked scans, ≥10 scans were averaged to minimize noise and to eliminate random peaks.

Since our VG ZABSpec was taken out of use, the mass spectrum of **11** was measured on a Bruker micrOTOF-Q ESI-HRMS instrument (Bruker Daltonics, Bremen, Germany). Mass spectrometer was controlled by Compass 1.3 for micrOTOF software package (Bruker Daltonics). The sample of **11** was dissolved in HPLC-grade acetonitrile (VWR International, Leuven, Belgium). The sample was then introduced to source using infusion pump. Positive ionization mode was used for MS analysis. The capillary voltage was maintained at –4500V and the end plate offset at –500 V. Nitrogen was used as nebulizer and drying gas. The pressure for the nebuliser gas was set at 0.4 bar. The drying gas flow rate was 4.0 L/min and the drying gas temperature 200°C. Mass detection was performed in the *m*/*z* range 50–1500. The resolving power of the mass spectrometer was typically 8000–12000. Sodium formate clusters were used for external calibration of the *m/z* range. Compass DataAnalysis 4.0 (Bruker Daltonics) was used for interpreting the mass data.

For collision induced dissociation (CID) MS/MS measurements, the collision energy in the m/z range 50–1500 varied from 20 eV or from 30 eV (m/z 50) to 75 eV (m/z 1500). Argon was used as collision gas. The mass spectrometer was operated in data-dependent mode to automatically select the most abundant precursor ions.

Table 6. Composition of the molecular ions

	$M^{+\bullet}$	Calcd	Obsd		$M^{+\bullet}$	Calcd	Obsd
11	$C_{18}H_{24}N_2O_3^{+\bullet}$	316.1787	316.1780	**17**	$C_{21}H_{22}N_2O_3^{+\bullet}$	350.1630	350.1631
13	$C_{19}H_{26}N_2O_3^{+\bullet}$	330.1943	330.1938	**18**	$C_{27}H_{26}N_2O_3^{+\bullet}$	426.1943	426.1940
14	$C_{24}H_{28}N_2O_3^{+\bullet}$	392.2100	392.2104	**19**	$C_{22}H_{24}N_2O_3^{+\bullet}$	364.1790	364.1781
12	$C_{23}H_{26}N_2O_3^{+\bullet}$	378.1943	378.1931	**20**	$C_{28}H_{28}N_2O_3^{+\bullet}$	440.2100	440.2093
15	$C_{23}H_{26}N_2O_3^{+\bullet}$	392.2100	392.2102	**22**	$C_{25}H_{22}N_2O_3^{+\bullet}$	398.1630	398.1612
16	$C_{25}H_{30}N_2O_3^{+\bullet}$	406.2256	406.2248				

Preparation of the starting materials

2-Benzyloxycarbonylamino-*N*-[2-(3,4-dimethoxyphenyl)ethyl]propanamide (6)

To a stirred and ice-salt bath-cooled solution of *N*-benzyloxycarbonyl-DL-alanine (**5**, 11.16 g, 0.05 mol) and triethylamine (5.06 g, 0.05 mol) in anhydrous toluene (150 mL), ethyl chloroformate (5.43 g, 0.05 mol) was added dropwise at a rate low enough to keep the internal temperature below –10 °C. After 5 min, a solution of homoveratrylamine (9.06 g, 0.05 mol) in CH_2Cl_2 (50 mL) was added dropwise, the internal temperature being kept below 0 °C. When the addition was complete, the reaction mixture was heated under reflux for 5 min. The mixture was allowed to cool down to room temperature and $CHCl_3$ (250 mL) was added. The mixture was next washed with saturated $NaHCO_3$ solution (3 × 75 mL) and water (2 × 75 mL), and then dried (Na_2SO_4), and the solvent was removed *in vacuo* to give a crude oily product, which crystallized on treatment with Et_2O. The crystals were filtered off, washed with Et_2O and recrystallized from EtOAc.

White crystalline substance, yield: 15.30 g (79%); mp 126-128 °C. ^{1}H NMR (400 MHz, $CDCl_3$): δ_H 1.34 (3H, d, J = 7.0 Hz, C*H*$_3$), 2.66-2.77 (2H, m, ArC*H*$_2$), 3.36-3.54 (2H, m, NC*H*$_2$), 3.84 (3H, s, OC*H*$_3$), 3.86 (3H, s, OC*H*$_3$), 4.08-4.18 (m, 1H, NC*H*), 5.08 (2H, dd, OC*H*$_2$, *J* = 18,6, 12,2 Hz), 5.30 (1H, br s, N*H*), 6.09 (1H, br s, N*H*), 6,70 (2H, br s, C_6*H*$_3$), 6.79 (1H, d, *J* = 8,3 Hz, C_6*H*$_3$), 7.28-7.38 (5H, m, C_6*H*$_5$). ^{13}C NMR (100 MHz, $CDCl_3$): δ_C 19.1, 35.6, 41.3, 51.0, 56.2, 56.3, 67.3, 111.9, 112.5, 121.1, 128.4, 128.6, 128.9, 131.8, 136.6, 148.1, 149.5, 156.4, 172.9**.** Anal. Calcd. for $C_{21}H_{26}N_2O_5$ C, 65.27; H, 6.78; N, 7.25; Found C, 65.02; H, 6.49; N, 7.13%.

1-[1′-(Benzyloxycarbonylamino)ethyl]-6,7-dimethoxy-3,4-dihydroisoquinoline (7)

To a stirred solution of the amide **6** (15.00 g, 38.8 mmol) in dry $CHCl_3$ (300 mL), $POCl_3$ (18.00 g, 117.4 mmol) was added. The mixture was heated under reflux for 3 h, and then evaporated *in vacuo*. The oily residue was dissolved in water (250 mL) under gentle warming, and the solution was cooled and extracted with EtOAc (2 × 75 mL). The aqueous phase was made alkaline with 25% NaOH solution with cooling, and extracted with $CHCl_3$ (4 × 150 mL). The combined organic extracts were dried (Na_2SO_4) and evaporated to give an oily product, which crystallized on treatment with Et_2O. The crystalline product was filtered off, washed with Et_2O and used in the next step without further purification.

Yield: 10.69 g (75%). An analytical sample of **7** was recrystallized from *i*Pr_2O to give beige crystals, mp 88-89 °C. ^{1}H NMR (400 MHz, $CDCl_3$): δ_H 1.39 (3H, d, *J* = 6.6 Hz, C*H*$_3$), 2.52-2.70

(2H, m, ArCH_2), 3.33-3.47 (1H, m, NCH_2), 3.78-3.95 (7H, m, NCH_2, 2 × OCH_3), 4.95-5.04 (1H, m, NCH_2), 5.14 (2H, dd, *J* = 15.4, 12.3 Hz, OCH_2), 6.47 (1H, d, *J* = 6.4 Hz, N*H*), 6.71 (1H, s, C_6H_2), 6.98 (1H, s, C_6H_2), 7.27-7.38 (5H, m, C_6H_5). ^{13}C NMR (100 MHz, $CDCl_3$): δ_C 21.6, 26.2, 46.8, 48.6, 56.4, 56.7, 66.8, 108.6, 111.1, 120.0, 128.3, 128.4, 128.8, 132.3, 137.3, 148.2, 151.6, 156.1, 166.0. Anal. Calcd. for $C_{21}H_{24}N_2O_4$ C, 68.46; H, 6.57; N, 7.60; Found C, 68.22; H, 6.41; N, 7.47%.

(1*S,1′*S**)-1-[1′-(Benzyloxycarbonylamino)ethyl]-6,7-dimethoxy-1,2,3,4-tetrahydroisoquinoline (8a)**

To a stirred and ice-cooled solution of dihydroisoquinoline **7** (10.00 g, 27.1 mmol) in MeOH (200 mL), $NaBH_4$ (3.10 g, 82 mmol) was added in small portions. The resulting mixture was stirred for 3 h with ice-water bath cooling and for 3 h at ambient temperature, and then evaporated *in vacuo*. The residue was dissolved in 5% HCl (150 mL), and the solution was made alkaline with 20% NaOH while cooled, and then extracted with $CHCl_3$ (4 × 150 mL). The combined organic extracts were dried (Na_2SO_4) and evaporated *in vacuo* to give an oily product, containing diastereomers **8a** and **8b** in a *ca.* 8 : 1 ratio. The oil crystallized on treatment with a 2:1 mixture of *n*-hexane and Et_2O. The crystalline product, which was filtered off and washed with *n*-hexane, proved to be diastereomerically pure **8a**. The crude crystalline product was used in the next step without further purification.

Yield: 7.42 g (74%). An analytical sample of **8a** was recrystallized from Et_2O to give a white crystalline substance, mp 68-70 °C. ^{1}H NMR (400 MHz, $CDCl_3$): δ_H 1.35 (d, 3H, *J* = 6.8 Hz, CH_3), 2.50-2.60 (m, 1H, ArCH_2), 2.72-2.83 (m, 1H, ArCH_2), 2.88-2.96 (m, 1H, NCH_2), 3.32-3.55 (m, 2H, NCH_2, NC*H*), 3.83 (s, 3H, OCH_3), 3.85 (s, 3H, OCH_3), 4.02 (br s, 1H, NC*H*), 4.97-5.05 (m, 1H, OCH_2), 5.54 (br s, 1H, N*H*), 6.58 (s, 1H, C_6H_2), 6.68 (s, 1H, C_6H_2), 7.28-7.34 (m, 5H, C_6H_5). ^{13}C NMR (100 MHz, $CDCl_3$): δ_C 19.0, 30.0, 43.2, 56.2, 56.4, 59.8, 66.6, 109.4, 112.0, 127.0, 128.0, 128.2, 128.5, 128.9, 137.3, 147.8, 147.9, 156.5. Anal. Calcd. for $C_{21}H_{26}N_2O_4$ C, 68.09; H, 7.07; N, 7.56; Found C, 67.76; H, 6.88; N, 7.24%.

(1*S,1′*S**)-1-(1′-Aminoethyl)-6,7-dimethoxy-1,2,3,4-tetrahydroisoquinoline dihydrobromide (9.2HBr)**

A mixture of compound **8a** (6.50 g, 17.5 mmol) and 33% HBr in AcOH (20 mL) was heated gently in a flask equipped with a $CaCl_2$ tube, with occasional shaking, until all of the substance had dissolved. The bubbling solution was left to stand at ambient temperature for 30 min, and Et_2O (25 mL) was then added. The yellow crystals of the dihydrobromide of **9** which formed were filtered off, washed with EtOAc and Et_2O, dried and recrystallized from 95% MeOH–Et_2O.

Beige crystalline substance, yield: 5.78 g (83%), mp 268-271 °C. ^{1}H NMR (400 MHz, D_2O): δ_H 1.46 (3H, d, *J* = 7.0 Hz, CH_3), 2.98-3.17 (2H, m, ArCH_2), 3.37-3.48 (1H, m, NCH_2), 3.63-3.73 (1H, m, NCH_2), 3.88 (6H, s, 2 × OCH_3), 4.25-4.36 (1H, m, NC*H*), 4,91 (1H, d, *J* = 4.9 Hz, NC*H*), 6.94 (1H, s, C_6H_2), 6.98 (1H, s, C_6H_2). ^{13}C NMR (100 MHz, D_2O): δ_C 24.5, 40.7, 49.3, 56.4, 56.6, 57.3, 110.4, 113.0, 118.9, 126.7, 148.3, 149.6. Anal. Calcd. for $C_{13}H_{22}Br_2N_2O_2$ C, 39.22; H, 5.57; N, 7.04; Found C, 38.87; H, 5.20; N, 6.98 %.

Pure diamine base **9** was obtained from the above dihydrobromide by alkaline treatment (20% NaOH), extraction (CH_2Cl_2) and evaporation under reduced pressure. The free base was dried in a vacuum desiccator for 24 h before further transformations.

General procedure for the preparation of tetra-, penta- and hexa-cyclic lactams 11-20 and 22

A mixture of diamine **9** or **10** or **21** (3 mmol) and the corresponding γ- or δ-oxo acid (3 mmol) was refluxed in toluene (40 mL) until no more starting materials could be detected by TLC (3-12 h). In case of **21**, some crystals of *p*-toluenesulfonic acids were also added to the reaction mixture prior to reflux. The solvent was then evaporated off and the oily or solid residue (the NMR spectrum of which was applied for determination of the diastereomeric ratios) was purified by means of column chromatography.

The ^{1}H NMR (**11**, **16–18**: 400 MHz; **12–15**, **19–20**, **22**: 500 MHz, $CDCl_3$) and ^{13}C NMR (100 MHz, $CDCl_3$) data of compounds **11–20** and **22** are presented in Tables 1–3.

8,9-Dimethoxy-3a,11-dimethyl-3,3a,5,6,10b,11-hexahydropyrrolo[2',1':2,3]imidazo[5,1-*a*]-isoquinolin-1(2*H*)-one (11). Eluent: EtOAc : MeOH = 4 : 1, yield: 0.73 g (77%), white crystalline substance, mp 192-193 °C (EtOAc). MS/MS from $[M+H]^+$ (33.57–41.03 eV): 220 (9), 205 (20), 204 (30), 202 (13), 193 (16), 192 (98), 190 (62), 189 (20), 177 (55), 176 ((94), 174 (100), 162 (20), 160 (26), 159 (25), 148 (68), 147 (21), 146 (18), 145 (19), 133 (10), 131 (48), 130 (10), 129 (10), 126 (12), 117 (12), 115 (9), 105 (7), 98 (14). Anal. Calcd. for $C_{18}H_{24}N_2O_3$ C, 68.33; H, 7.65; N, 8.85; Found C, 68.09; H, 7.48; N, 8.72%.

8,9-Dimethoxy-11-methyl-3a-phenyl-3,3a,5,6,10b,11-hexahydropyrrolo[2',1':2,3]imidazo-[5,1-*a*]isoquinolin-1(2*H*)-one (12). Eluent: EtOAc, yield: 0.77 g (68%), beige solid, mp 155-158 °C. Anal. Calcd. for $C_{23}H_{26}N_2O_3$ C, 72.99; H, 6.92; N, 7.40; Found C, 72.82; H, 6.75; N, 7.27%.

8,9-Dimethoxy-3a,11-dimethyl-3,3a,5,6,11,12-hexahydro-10b*H*-pyrrolo[2',1':2,3]pyrimido-[6,1-*a*]isoquinolin-1(2*H*)-one (13): Eluent: EtOAc, yield: 0.58 g (59%), beige crystalline substance, mp 139-141 °C. Anal. Calcd. for $C_{19}H_{26}N_2O_3$ C, 69.06; H, 7.93; N, 8.48; Found C, 68.85; H, 7.62; N, 8.30%.

8,9-Dimethoxy-11-methyl-3a-phenyl-3,3a,5,6,11,12-hexahydro-10b*H*-pyrrolo[2',1':2,3]pyrimido[6,1-*a*]isoquinolin-1(2*H*)-one (14). Eluent: EtOAc, yield: 0.76 g (65%), white crystalline substance, mp 233-234 °C (*i*Pr_2O–EtoAc). Anal. Calcd. for $C_{24}H_{28}N_2O_3$ C, 73.44; H, 7.19; N, 7.14; Found C, 73.19; H, 7.03; N, 6.98%.

9,10-Dimethoxy-12-methyl-4a-phenyl-2,3,4,4a,6,7,11b,12-octahydro-1*H*-pyrido[2',1':2,3]-imidazo[5,1-*a*]isoquinolin-1-one (15). Eluent: EtOAc, yield: 0.74 g (63%), beige solid, mp 174-177 °C. Anal. Calcd. for $C_{24}H_{28}N_2O_3$ C, 73.44; H, 7.19; N, 7.14; Found C, 73.61; H, 7.06; N, 7.12%.

9,10-Dimethoxy-12-methyl-4a-phenyl-2,3,4,4a,6,7,12,13-octahydro-1*H*,11b*H*-pyrido-[2',1':2,3]pyrimido[6,1-*a*]isoquinolin-1-one (16). Eluent: EtOAc, yield: 0.63 g (52%), white crystalline substance, mp 202-204 °C. Anal. Calcd. for $C_{25}H_{30}N_2O_3$ C, 73.86; H, 7.44; N, 6.89; Found C, 73.61; H, 7.38; N, 6.62%.

2,3-Dimethoxy-5-methyl-4b,5,13,14-tetrahydroisoindolo[1',2':2,3]imidazo[5,1-*a*]iso-quinolin-7(11b*H*)-one (17). Eluent: EtOAc, yield: 0.78 g (74%), white crystalline substance, mp 186-187 °C. Anal. Calcd. for $C_{21}H_{22}N_2O_3$ C, 71.98; H, 6.33; N, 7.99; Found C, 72.15; H, 6.10; N, 7.82%.

2,3-Dimethoxy-5-methyl-11b-phenyl-4b,5,13,14-tetrahydroisoindolo[1',2':2,3]imidazo-[5,1-*a*]isoquinolin-7(11b*H*)-one (18). Eluent: EtOAc, yield: 0.81 g (63%), white crystalline substance, mp 174-175 °C (Et_2O). Anal. Calcd. for $C_{27}H_{26}N_2O_3$ C, 76.03; H, 6.14; N, 6.57; Found C, 76.26; H, 6.02; N, 6.49%.

2,3-Dimethoxy-5-methyl-5,6,14,15-tetrahydro-4b*H*-isoindolo[1',2':2,3]pyrimido[6,1-*a*]iso-quinolin-8(12b*H*)-one (19). Eluent: EtOAc, yield: 0.83 g (76%), white crystalline substance, mp 209-210 °C (*i*Pr_2O–EtOAc). Anal. Calcd. for $C_{22}H_{24}N_2O_3$ C, 72.50; H, 6.64; N, 7.69; Found C, 72.26; H, 6.41; N, 7.74%.

2,3-Dimethoxy-5-methyl-12b-phenyl-5,6,14,15-tetrahydro-4b*H*-isoindolo[1',2':2,3]pyrimi-do[6,1-*a*]isoquinolin-8(12b*H*)-one (20). Eluent: EtOAc, yield: 0.77 g (58%), beige solid, mp 225-227 °C (*i*Pr_2O–EtOAc). Anal. Calcd. for $C_{28}H_{28}N_2O_3$ C, 76.34; H, 6.41; N,3, 6.36; Found C, 76.10; H, 6.29; N, 6.14%.

2,3-Dimethoxy-16,17-dihydro-4b*H*-isoindolo[2,1-*a*]isoquinolino[2,1-*c*]quinazolin-10(14b*H*)-one (22). Eluent: EtOAc : MeOH 4 : 1, yield: 0.72 g (60%), white crystalline substance, mp 245-246 °C (EtOAc–EtOH). Anal. Calcd. for $C_{25}H_{22}N_2O_3$ C, 75.36; H, 5.57; N, 7.03; Found C, 75.42; H, 5.39; N, 6.84%.

Acknowledgements

ZZ and LL thank TÁMOP-4.2.1/B-09/1/KONV-2010-0005 for financial support.

References and Notes

1. (a) Meyers, A. I.; Brengel, G. P. *Chem. Commun.* **1997**, 1. (b) Csende, F.; Stájer, G. *Heterocycles* **2000**, *53*, 1379. (c) Csende, F.; Stájer, G. *Curr. Org. Chem.* **2005**, *9*, 1261.
2. (a) Tietze, L. F. *Chem. Rev.* **1996**, *96*, 115. (b) Tietze, L. F.; Rackelmann, N. *Pure Appl. Chem.* **2004**, *76*, 1967. (c) Padwa, A.; Bur, S. K. *Tetrahedron* **2007**, 63, 5341. (d) Alba, A.-N.; Companyo, X.; Viciano, M.; Rios, R. *Curr. Org. Chem.* **2009**, *13*, 1432.
3. (a) Meyers, A. I.; Downing, S. V.; Weiser, M. J. *J. Org. Chem.* **2001**, *66*, 1413. (b) Lázár, L.; Fülöp, F. *Eur. J. Org. Chem.* **2003**, 3025.
4. (a) Groaning, M. D.; Meyers, A. I. *Tetrahedron* **2000**, *56*, 9843. (b) Escolano, C.; Amat, M.; Bosch J. *Chem. Eur. J.* **2006**, *12*, 8198. (c) Amat, M.; Perez, M.; Bosch, J. *Synlett* **2011**, 143. (d) Amat, M.; Arróniz, C.; Molins, E.; Escolano, C.; Bosch, J. *Org. Biomol. Chem.* **2011**, *9*, 2175.

5. (a) Lázár, L; Kivelä, H.; Pihlaja, K.; Fülöp, F. *Tetrahedron Lett.* **2004**, *45*, 6199. (b) Kivelä, H.; Tähtinen, P.; Martiskainen, O.; Pihlaja, K.; Lázár, L.; Vigóczki, E.; Fülöp, F. *J. Mol. Struct.* **2010**, *983*, 62.
6. (a) Zalán, Z.; Martinek, T. A.; Lázár, L.; Sillanpää, R., Fülöp, F. *Tetrahedron* **2006**, *62*, 2883. (b) Schuster, I.; Koch, A.; Heydenreich, M.; Kleinpeter, E.; Forró, E.; Lázár, L.; Sillanpää, R.; Fülöp, F. *Eur. J. Org. Chem.* **2008**, 1464. (c) Kleinpeter, E., Szatmári, I.; Lázár, L., Koch, A.; Heydenreich, M.; Fülöp, F. *Tetrahedron* **2009**, *65*, 8021. (d) Vigóczki, E., Hetényi, A., Lázár, L.; Fülöp, F. *ARKIVOC* **2009**, (*xii*), 8.
7. Zalán, Z.; Martinek, T. A.; Lázár, L.; Fülöp, F. *Tetrahedron* **2003**, *59*, 9117.
8. von Nussbaum, F.; Miller, B.; Wild, S.; Hilger, C. S.; Schumann, S.; Zorbas, H.; Beck, W.; Steglich, W. *J. Med. Chem.* **1999**, *42*, 3478.
9. All of the prepared compounds are racemic. For a better stereochemical comparison of the polycyclic lactams, diamine **9** was depicted on the Schemes as (1S*,1′*S**), while **10** as (1*R**,1′*R**) diastereomer.

